Remote Sensing of Environment 132 (2013) 32–39

Contents lists available at SciVerse ScienceDirect

Remote Sensing of Environment

journal homepage: www.elsevier.com/locate/rse

The potential of dual-wavelength laser scanning for estimating vegetation moisture content

R. Gaulton [a,*], F.M. Danson [b], F.A. Ramirez [b], O. Gunawan [b]

[a] School of Civil Engineering and Geosciences, Cassie Building, Newcastle University, Newcastle upon Tyne NE1 7RU, United Kingdom
[b] School of Environment and Life Sciences, University of Salford, Salford M5 4WT, United Kingdom

ARTICLE INFO

Article history:
Received 5 September 2012
Received in revised form 2 January 2013
Accepted 5 January 2013
Available online xxxx

Keywords:
Salford Advanced Laser Canopy Analyser
Leaf water content
Leaf optical properties
Spectral indices
Leaf biochemistry
Multispectral LiDAR

ABSTRACT

Vegetation moisture content is an important early indicator of forest drought stress, disease and fire risk. Existing remote sensing techniques to measure biochemical properties of vegetation, such as Equivalent Water Thickness (EWT), are limited by an inability to differentiate canopy and understorey properties and are influenced by variations in canopy structure. By providing a range-resolved estimate of reflectance, laser scanner measurements have the potential to overcome these limitations. Dual-wavelength laser scanning can provide an active measurement of reflectance from which spectral indices can be derived that are insensitive to range, incidence angle and scattering area of the target within the laser beam, factors that make exploiting single-wavelength laser scanner intensity data difficult.

This study demonstrates the potential of dual-wavelength laser scanning for measurement of leaf biochemical properties, through determining the relationship between a laser-scanner-derived spectral index, using near infrared (1063 nm) and middle infrared (1545 nm) wavelengths, and the EWT of individual leaves. The suitability and sensitivity of the index is tested using a leaf optical properties model (PROSPECT-5) and the method is tested experimentally under laboratory conditions using the Salford Advanced Laser Canopy Analyser. A strong relationship (R^2 = 0.8, RMSE = 0.0069 g cm^{-2}) was found between a normalised ratio of the two wavelengths and measured EWT of leaf samples. The relationship corresponds well to that predicted by modelling. However, the experimental data also revealed significant spatial variability in the index value across individual leaves, suggesting heterogeneity in moisture distribution at within-leaf scales. The study suggests significant potential for using dual-wavelength and multispectral laser scanning for measuring vegetation biochemical properties.

1. Introduction

The lack of adequate data on forest health status has been identified as a key information gap in understanding climate change risks for forests (Allen et al., 2010). Recent increases in tree mortality caused by drought suggest that climatic factors may already be resulting in forest die-back in some regions (e.g. southern parts of Europe), with potential for a conversion to fire-prone, scrub or savannah vegetation (Allen et al., 2010; Nepstad et al., 2008). In addition, global spread of non-native tree pathogens and pests is occurring and climate changes are leading to an alteration in host and pathogen distributions and host susceptibility (Sturrock et al., 2011). Early detection is often vital in reducing spread of infections and methods to detect early symptoms of disease, including water stress and defoliation, are likely to be of major benefit to forest management by improving the chances of control or eradication (Meentemeyer et al., 2008).

Leaf or vegetation moisture content is typically measured as Equivalent Water Thickness (EWT, the weight of water per unit area of leaf) and is an essential early indicator of forest drought stress (Zarco-Tejada et al., 2003), infection by tree diseases and forest pests, such as Mountain Pine Beetle (Skakun et al., 2003), and is of key importance as an input to models of forest fire susceptibility, ignition and propagation (Danson & Bowyer, 2004). Leaf moisture content also has potential applications in assessing drought risk and irrigation needs in agricultural crops (Rodríguez-Pérez et al., 2006; Wang et al., 2012; Yi et al., 2012), whilst the moisture content of fuels plays a role in determining fire risk in a variety of other ecosystems, such as Mediterranean-climate shrublands (Peterson et al., 2008). Whilst a range of existing direct physiological approaches can be used to measure vegetation stress and EWT in the field, the scope of such approaches for examining temporal and spatial heterogeneity and for long-term monitoring is limited. Vegetation and soil moisture content can be measured over large spatial and long temporal scales using a range of remote sensing techniques, including radar, thermal and optical sensors. A number of spectral indices based on near infrared (NIR) and middle infrared (MIR) wavelengths have been developed that strongly relate to EWT (Ceccato et al., 2001) and these have been widely applied to satellite data (e.g. Landsat 5 TM) for measuring vegetation liquid water content, for drought assessment, and for disease detection (Gao, 1996; Gu et al., 2007; Skakun et

* Corresponding author. Tel.: +44 191 222 6577; fax: +44 191 222 6502.
E-mail address: rachel.gaulton@ncl.ac.uk (R. Gaulton).

0034-4257/$ – see front matter © 2013 Elsevier Inc. All rights reserved.
http://dx.doi.org/10.1016/j.rse.2013.01.001

al., 2003). The accessibility, high spatial and temporal resolution, and presence of a long archive of optical imagery gives such approaches an advantage over the use of radar imagery for long-term monitoring. However, passive optical measurements of canopy reflectance, and resulting estimates of leaf biochemical properties (including EWT, but also for example, leaf pigment concentrations), are influenced by atmospheric conditions, illumination and viewing geometry, canopy structure, and soil and understorey vegetation reflectance (e.g. Asner, 1998; Dawson et al., 2003; Huete et al., 1985; Wessman, 1994). It is particularly difficult to separate the vegetation canopy signal from that of the background understorey and soil, a problem frequently shared with synthetic aperture radar (e.g. Notarnicola & Posa, 2007) and thermal measurements (e.g. Thomson et al., 2012).

Active measurements of reflectance, derived from laser scanner data, have the potential to overcome many of these limitations. Active measurements, utilising a laser illumination source, are largely independent of illumination conditions (potentially allowing measurements at night) and make reflectance measurements with a fixed and optimal viewing and illumination geometry, measuring backscatter at the 'hotspot' where no shadowing is present (Woodhouse et al., 2011). As the measurements are range resolved, these approaches also have a significant benefit in providing three-dimensional estimates of reflectance properties of targets and, based on modelling studies, in separating, by range, reflectance signals of tree canopies and the understorey and soil (Morsdorf et al., 2009; Woodhouse et al., 2011). In three-dimensional and heterogeneous environments such as forests, such methods therefore have great promise in improving estimates of canopy leaf biochemical properties and providing more direct measurement of soil properties and shaded understorey. Measurements from terrestrial laser scanners are required to improve the exploitation of satellite data, through facilitating the up-scaling of leaf level measurements to the canopy (for example, Van der Zande et al., 2009) and the measurement of spatial heterogeneity in canopy properties. Airborne and satellite-based systems have the potential to allow improved estimates of forest and vegetation vigour over larger areas.

Terrestrial and airborne laser scanning has been widely utilised for the retrieval of forest structure parameters (for comprehensive reviews see Hyyppä et al. (2008) and Van Leeuwen and Nieuwenhuis (2010)). However, little consideration has been given to the use of intensity data from laser scanners to provide complementary information on leaf biochemistry and vegetation type. A number of studies have attempted to utilise laser scanner intensity data for species classification or distribution mapping in forested environments, usually in conjunction with structural indices (for example, Kim et al., 2011; Korpela, 2008; Ørka et al., 2009) and other researchers have focused on fusion of laser scanner and passive hyperspectral data sets to obtain both physical and biochemical properties of vegetation canopies (for example, Asner et al., 2007). A small number of recent studies have examined the ability of terrestrial laser scanner data to provide information on leaf biochemical properties (Eitel et al., 2010, 2011; Wei et al., 2012). Eitel et al. (2010), showed a strong correlation between laser return intensity (at 532 nm) and Chlorophyll a and b (Chl_{ab}) content, but also demonstrated that estimation of Chl_{ab} levels were significantly influenced by incidence angle of the laser beam and by the presence of 'edge returns', where the leaf only partially occupied the laser footprint. Correction for incidence angle effects in vegetation canopies, which are dependent on leaf angle distribution, is extremely difficult with a single-wavelength laser system.

A detailed review of calibration considerations for laser intensity data is beyond the scope of this paper, but can be found in Höfle and Pfeifer (2007) and Kaasalainen et al. (2009). However, the exploitation of intensity data for determining target reflectance properties is complicated by the dependence of backscatter intensity on the range to the target, the scattering area of the target within the laser beam, and the local incidence angle and surface roughness of the target (Ahokas et al., 2006; Höfle & Pfeifer, 2007; Kaasalainen et al., 2009). As range information for each return is also acquired by laser scanners, this can be used, in conjunction with knowledge of the instrument characteristics, to calibrate for range effects based on the inverse distance square law (Ahokas et al., 2009). Correcting for local incidence angle and for returns resulting from objects partially occupying the laser beam is more difficult. The use of dual-wavelength laser scanning systems potentially allows the calculation of spectral ratios that account for these factors. The influence of incidence angle and area of the target within the footprint will be similar at both wavelengths and so, assuming the beams are perfectly aligned, the resulting ratio should be insensitive to these factors and influenced primarily by the spectral reflectance of the target. Such systems therefore hold significant promise for leaf biochemical measurements in vegetation canopies (Eitel et al., 2010, 2011). Through modelling approaches, Morsdorf et al. (2009) demonstrated the potential of multispectral laser scanning to detect variation in chlorophyll content. Range resolved measurements of canopy biochemical properties were also shown theoretically to facilitate separation of responses from woody material and foliage (Morsdorf et al., 2009).

A number of prototype, mainly laboratory-based, multispectral laser systems have recently been developed for vegetation applications. Rall and Knox (2004) developed the dual-wavelength Spectral Ratio Biospheric Lidar, showing changes in the red to near-infrared ratio from a tree canopy over a phenological cycle. Tan et al. (2005) developed a dual-wavelength (1064 nm and 532 nm) airborne system (the Multiwavelength Airborne Polarimetric Lidar), demonstrating reflectance differences between tree species were detectable, whilst Woodhouse et al. (2011) have developed the Multispectral Canopy LiDAR system, which uses a single tunable laser aimed at measuring Normalised Difference Vegetation Index (NDVI) and Photochemical Reflectance Index (PRI) and is designed as a prototype airborne sensor. Wei et al. (2012) describe a laboratory-based prototype of a multispectral LiDAR designed for vegetation applications and making measurements at four wavelengths (556, 670, 700 and 780 nm). Hakala et al. (2012) describe a multispectral LiDAR system using supercontinuum lasers capable of making measurements in 8 spectral bands optimised for vegetation. None of these systems are easily field portable and only the latter two (Hakala et al., 2012 and Wei et al., 2012) contain a scanning mechanism, limiting their immediate usefulness and practicality for in-situ measurements of vegetation canopies.

Narayanan and Pflum (1999) demonstrated the potential of ratios of laser reflectance in the 9–11 μm wavelength region for distinguishing stressed and healthy plants, but did not relate the ratios to specific biochemical properties and were largely unable to distinguish the type of stress. Only one study has experimentally examined the potential of dual-wavelength or multispectral laser scanning to measure leaf biochemical properties and none have examined the estimation of leaf water content. Wei et al. (2012) demonstrated strong relationships (R^2 of up to 0.82) between actively measured spectral indices, including an NDVI equivalent, and foliage nitrogen levels, using data derived from their four-wavelength laser scanner. Their results showed that multispectral laser scanners have significant potential for measurement of leaf biochemical properties, but the study was based on a very small number of samples and further research is needed to demonstrate the full potential of such techniques and to explore the range of biochemical properties that can be retrieved.

This paper tests the potential of a unique, full-waveform dual-wavelength laser scanner system, the Salford Advanced Laser Canopy Analyser (SALCA), for estimating the EWT of leaf samples. The field-portable SALCA instrument (Section 2.1) operates at two wavelengths (1063 nm and 1545 nm), scans a full hemisphere, and is the first such instrument to include a middle-infrared wavelength. SALCA therefore has significant potential for providing an improved ground-based approach to measurement of canopy EWT, as a validation instrument for other remotely sensed data sets, allowing up-scaling of leaf level physiological measurements to canopy scales, and as a proof-of-concept for future airborne or satellite-based systems designed to monitor forest vigour. The specific aims of this study are to i) determine the suitability and sensitivity of SALCA wavelengths for measurement of leaf moisture content in comparison to more commonly employed spectral indices and ii) to provide the first experimental demonstration of the potential of dual-wavelength laser scanning to measure leaf moisture content.

2. Methods

The aims of the paper are addressed using a combination of radiative transfer modelling and experimental approaches. The PROSPECT-5 leaf optical properties model (Féret et al., 2008; Jacquemoud & Baret, 1990) was used to compare SALCA-wavelength derived spectral indices to those more commonly used in passive optical systems and determine their sensitivity to leaf moisture content. Measurements from SALCA were then used to determine the relationships between laser-derived reflectance, spectral indices and leaf EWT.

2.1. The Salford Advanced Laser Canopy Analyser

The SALCA instrument is a full-waveform terrestrial laser scanner designed for characterising forest canopies by the University of Salford, UK and Halo Photonics Ltd. This hemispherical-scanning instrument records the full-waveform of backscattered energy at two wavelengths in the near and middle infrared (1063 nm and 1545 nm). Near and middle infrared wavelengths were selected to allow separation of foliage and woody material which, along with the full waveform data generated, should improve estimates of forest LAI over those obtainable from commercially available laser scanner systems. The specific wavelength selection of 1063 nm and 1545 nm reflects the commercial availability of lasers at these wavelengths. However, the inclusion of near-infrared and middle-infrared wavelengths also allows the calculation of spectral indices comparable to those more commonly used with passive optical data for the estimation of leaf moisture content (Féret et al., 2011). The full specification of the instrument is given in Table 1. The two laser beams follow the same optical path and are closely aligned, with an offset between wavelengths (6 μrad), equating to less than 1% of the footprint area, caused by the speed of rotation of the scanner head and sequential firing of the wavelengths. External neutral density filters can be used to adjust signal levels to avoid near-range saturation or improve signal-to-noise ratios at long range.

2.2. Leaf reflectance modelling

The aim of the modelling component of this study was to determine the suitability of SALCA wavelengths for estimating leaf moisture content, in comparison to wavelengths and indices previously suggested for use in estimation of EWT, and to define the optimal form of a SALCA-derived spectral index for this purpose. However, it is not the intention of this paper to determine the optimal wavelengths for use in EWT estimation; that aim has been addressed elsewhere (for example, Féret et al., 2011; Wang & Li, 2012). The PROSPECT-5 leaf optical model was used to simulate a dataset of leaf spectral reflectance. A total of 420 model runs were used to simulate leaf reflectance over a range of EWT, dry matter content and leaf structure parameters (Table 2). Pigment concentration was kept constant (at model defaults of $C_{ab}=47.7$ μg cm^{-2}, $C_{ar}=4.4$ μg cm^{-2}, $C_{brown}=0$) as these parameters have no significant influence on the near-infrared and middle infrared reflectance of interest in this study. The minimum and maximum input values for the water content (denoted C_w in PROSPECT) and dry matter content (C_m) parameters were the minimum and maximum parameter values identified across four experimental datasets by Féret et al. (2008), including the LOPEX, CALMIT, ANGERS and HAWAII databases. The leaf structure parameter (N) covered the full range of 1 to 3 (Féret et al., 2008). A uniform distribution of parameter values was assumed, parameters were assumed to be independent (acknowledged to be unlikely in reality) and all combinations of parameters were considered.

Leaf reflectance values corresponding closely to SALCA wavelengths (1063 and 1545 nm) were extracted from the simulated dataset and used to calculate values of two potential spectral indices, a normalised ratio (SALCA Normalised Ratio Index, SNRI) and a simple ratio (SALCA Simple Ratio Index, SSRI) (Table 3). In addition, two commonly used indices based on other wavelengths (the Normalised Difference Water Index (NDWI) and the Moisture Stress Index (MSI)), and two indices shown to be optimal by Féret et al. (2011), $ND_{1062,\ 1393}$ and $RI_{1062,\ 1393}$, were calculated to allow comparison of sensitivity (Table 3). The choice of such indices was limited to indices using ratios of discrete bands rather than including those using approaches, such as derivative analysis, which would require hyperspectral data that is unavailable from SALCA.

Relationships between the simulated spectral index values and EWT (defined as the value of the PROSPECT C_w parameter) were determined using Reduced Major Axis (RMA) regression, due to the need for symmetrical relationships that can be inverted to estimate biochemical parameters (Smith, 2009). Spectral indices and biochemical parameters were square root transformed prior to regression to ensure a linear relationship. RMA was then used to obtain regression coefficients and coefficients of determination (R^2) which provided the basis to assess the relative sensitivity of the spectral indices to leaf EWT. The Root Mean Square Error (RMSE) of the relationships in predicting biochemical parameters was determined by inverting the derived models and estimating RMSE using leave-one-out cross validation methods. Relationships with the other biochemical parameters (C_m and N) were also assessed for SALCA-derived indices to determine their likely influence on estimation of EWT. All statistical analysis was implemented in MATLAB® (R2012a, The MathWorks, Natick, MA).

2.3. EWT retrieval from SALCA data

2.3.1. Experimental setup

To determine the relationship between SALCA return intensity and leaf EWT, five leaves, from three different species, were chosen on the basis of availability, having a large leaf area, and representing a range of potential leaf structures. One leaf was *Brassica oleracea* (cabbage), one a *Spathiphyllum* species (peace lily) and the remaining three were *Fallopia japonica* (Japanese knotweed). In the case of one of the *Fallopia* samples, two leaves were used to provide a double thickness and ensure a high level of EWT for comparative purposes. The fresh leaves were

Table 1
System characteristics of the SALCA instrument.

SALCA system specifications:	
Centre wavelengths	1545.4 nm and 1063.4 nm
Pulse length	3 ns (1545 nm) and 1 ns (1063 nm)
Pulse rate	5 kHz
Beam width at sensor	3.6 mm (1545 nm) and 2.4 mm (1063 nm)
Beam divergence	0.56 mrad
Laser output energy	5 μJ (1545 nm) and 0.5 μJ (1063 nm)
Detector field of view	2.67 mrad
Sampling rate	1 GHz
Range resolution	15 cm
Maximum range	105 m
Angular sampling step	1.05 mrad
Angular displacement between wavelengths	6 μrad

Table 2
Model parameters used in PROSPECT-5 model simulations.

Prospect parameter	Minimum	Interval	Maximum
Equivalent water thickness (C_w), g cm^{-2}	0.0043	0.005	0.0713
Dry matter content (C_m), g cm^{-2}	0.0017	0.0025	0.0165
Leaf structure (N)	1	0.5	3

Table 3
Spectral reflectance indices considered in this study. ρ indicates reflectance and all wavelengths are given in nm.

Index	Formula	Source
SALCA Normalised Ratio Index	$SNRI = \frac{(\rho_{1063} - \rho_{1545})}{(\rho_{1063} + \rho_{1545})}$	This study
SALCA Simple Ratio Index	$SSRI = \frac{\rho_{1063}}{\rho_{1545}}$	This study
$ND_{1062,\ 1393}$	$ND_{1062,1393} = \frac{(\rho_{1062} - \rho_{1393})}{(\rho_{1062} + \rho_{1393})}$	Féret et al. (2011)
$RI_{1062,\ 1393}$	$RI_{1062,1393} = \frac{\rho_{1062}}{\rho_{1393}}$	Féret et al. (2011)
Normalised Difference Water Index	$NDWI = \frac{(\rho_{860} - \rho_{1240})}{(\rho_{860} + \rho_{1240})}$	Gao (1996)
Moisture Stress Index	$MSI = \frac{\rho_{1600}}{\rho_{820}}$	Rock et al. (1986)

first weighed and their leaf areas determined. They were then mounted in cardboard frames and supports to ensure consistent placement throughout the experiment and easy extraction of valid leaf data points from the laser scanner data. The frames, and a white Spectralon® calibration panel, were positioned at a distance of 6.05 m from the SALCA instrument, resulting in a beam footprint diameter of 0.58 cm at 1063 nm and 0.7 cm at 1545 nm. A clear space of 60 cm (four range bins) was ensured behind the samples so that leaf response was not influenced by transmitted energy reflected from the wall behind. The leaves were then scanned at 16 time intervals over a total period of 47 h as they dried naturally. An absorptive neutral density filter with optical density of 1.0 was used during the experiment to ensure the signal did not saturate the detector given the high reflectivity of the Spectralon panel and close range of samples. Each leaf sample (including mount) was weighed immediately before each scan to allow determination of EWT. To minimise any influence of instrument temperature or background illumination on intensity measurements, lights were switched off during scans and SALCA was turned on exactly eight minutes before each scan. At the end of the experiment, all leaf samples were oven dried for 48 h at 65 °C to determine dry weight and allow calculation of EWT.

2.3.2. SALCA data processing and analysis

Individual scans were processed to extract waveforms corresponding to each leaf sample. Between 12 and 35 waveforms were identified and extracted per leaf, avoiding waveforms close to the cardboard frame. As waveforms were extracted from within the frame, only waveforms representing full hits of the leaf (generating single returns) were included. The same waveforms, with consistent footprint locations on the leaf, were extracted for each time interval. A constant threshold was applied to eliminate parts of the waveform signal resulting from background noise by setting the intensity of these regions to zero. Backscatter intensity was then determined as the maximum intensity of the return peaks, which were located using zero crossings of the first derivative of the waveforms. As all returns were from single leaf targets occupying the entire laser footprint, integration of the area under the waveform curve was not necessary to provide a measure of intensity in this case.

As all leaf samples were at very similar ranges (within a single 15 cm range bin), correction of range effects on intensity was not necessary for this study. Intensity was normalised for variations in laser output intensity (which should vary by less than 5% of peak power) and background illumination, based on intensity values of 140 waveforms extracted from the Spectralon® panel (with a known reflectivity of 0.94 at 1063 nm and 0.96 at 1545 nm) included in each scan. Signal-to-noise ratios of the intensity data, for the Spectralon panel located at 6.05 m range and with the filter combinations used in this experiment, were 8.87 dB and 12.88 dB for the 1063 nm and 1545 nm wavelengths respectively. The SALCA instrument displayed some non-linearity in reflectance response, especially in the 1545 nm wavelength. Calibration of measured intensity to absolute reflectance was therefore necessary before calculation of indices. Empirical relationships between measured intensity and reflectance were fitted to calibration data obtained by scanning eight near-Lambertian calibration panels exhibiting a variety of reflectances (as measured with an ASD field spectroradiometer with a contact probe), at the same range as the experiment was conducted. These relationships, a quadratic relationship for 1063 nm (Eq. 1, $R^2 = 0.98$, RMSE = 0.048) and an exponential relationship for 1545 nm (Eq. 2, $R^2 = 0.96$, RMSE = 0.069), were then used to convert intensity measurements (I) to reflectance (ρ_{1063} and ρ_{1545}). The difference in the extent of non-linearity of the relationships reflects the significant difference in the outgoing pulse strength at the two wavelengths (Table 1) and therefore in the range of signal intensities recorded at the detector.

$$\rho_{1063=aI^2+bI+c} \text{ where } a = 4.68 \times 10^{-5}, b = 0.0063, c = -0.0667 \quad (1)$$

$$\rho_{1545=ae^{bI}+ce^{dI}} \text{ where } a = 1.82 \times 10^{-11}, b = 0.1056, c = 0.0233, \quad d = 0.0123 \quad (2)$$

Intensity values were extracted for each waveform from both wavelengths and SNRI and SSRI (Section 2.2) were calculated on a waveform-by-waveform basis. The mean and standard deviation of the index values, and of the individual wavelength reflectance values, were then calculated for each leaf sample at each time interval. RMA regression was again used to determine relationships (of all leaves combined) between reflectance at 1063 nm, reflectance at 1545 nm, spectral indices and the measured leaf EWT. As relationships with spectral indices were very close to linear for the experimental data, these variables were not square root transformed prior to analysis; however, in analysing reflectance of the individual wavelengths, transformation was applied. As above, RMSE was determined using leave-one-out cross validation.

3. Results

3.1. PROSPECT modelling

All of the spectral indices tested, including those derived using SALCA wavelengths, were found to be significantly correlated with EWT ($P < 0.05$, Table 4). The most strongly correlated index, with the lowest error in prediction, was $ND_{1062,1393}$, as proposed by Féret et al. (2011). However, the SALCA Normalised Ratio Index (SNRI) was also strongly related, with a similar R^2 value to $ND_{1062,1393}$ and the more commonly used NDWI, and slightly lower RMSE than NDWI. This SALCA-derived index therefore seems well suited (and the optimal form of index) for use in estimating EWT. The simple ratio of SALCA bands (SSRI), along with $RI_{1062,1393}$ and MSI, had a slightly weaker relationship to EWT and produced a slightly higher RMSE, but still represents a useful index.

The sensitivity of the SNRI to other PROSPECT model parameters was also evaluated. No statistically significant relationship was found with dry matter content (C_m), suggesting the index should be relatively insensitive to the amount of dry matter in a leaf. The relationship between the optimum index identified ($ND_{1062,1393}$) and dry matter content was also not significant. However, a significant, but weak,

Table 4
Sensitivity of spectral indices to EWT (g cm^{-2}) based on the RMSE in prediction, R^2 and significance of the regression.

Index	RMSE	R^2
SALCA Normalised Ratio Index	0.0076	0.8957**
SALCA Simple Ratio Index	0.0121	0.8017**
$ND_{1062,\ 1393}$	0.0071	0.9092**
$RI_{1062,\ 1393}$	0.0111	0.8311**
Normalised Difference Water Index	0.0080	0.8980**
Moisture Stress Index	0.0091	0.8717**

** Slope is significant at a $P < 0.01$ level.

relationship was found between the leaf structure parameter (N) and the SNRI (along with the $ND_{1062,1393}$ and MSI) with an increase in the value of N resulting in a small decrease in the value of the SNRI ($y = -0.5254x + 1.401$, $R^2 = 0.0818$). This indicates some residual impact of leaf structure on index values, in keeping with the influence found for other spectral indices involving the middle-infrared.

3.2. Experimental study

During the course of the experiment, the leaves dried at different rates and to different degrees (Fig. 1). The *Spathiphyllum* leaf was particularly resistant to drying, with EWT changing little during the course of the experiment. *B. oleracea* also dried relatively slowly and maintained high levels of EWT until the end of the experiment. However, all leaves combined provided a significant range of EWT values over time, from 0 $g\,cm^{-2}$ to 0.05 $g\,cm^{-2}$, similar to the range in the modelled data.

Statistically significant relationships were found between EWT and reflectance derived from active SALCA measurements at both wavelengths (Fig. 2). 1063 nm reflectance declined only slightly as EWT increased, whilst reflectance at 1545 nm decreased more significantly. Use of a single wavelength (1545 nm) to predict EWT resulted in a RMSE of 0.008 $g\,cm^{-2}$ (Table 5). A strong ($R^2 = 0.8$, RMSE = 0.0069 $g\,cm^{-2}$), almost linear relationship was found between the SALCA-derived SNRI and EWT (Fig. 3). Fitting a polynomial curve to the relationship resulted in no significant improvement in model performance compared to a linear relationship and the relationship between SNRI (as well as SSRI) and EWT was therefore modelled as linear (Table 5). As predicted by PROSPECT, the SNRI showed a slightly stronger relationship to EWT than SSRI and both resulted in a decrease in the error of estimation of EWT over the use of a single wavelength (Table 5). At the level of a single species, relationships between EWT and SNRI were somewhat weaker but still resulted in statistically significant relationships ($R^2 = 0.743$ and RMSE = 0.0059 $g\,cm^{-2}$ for *B. oleracea* and $R^2 = 0.656$ and RMSE = 0.0075 $g\,cm^{-2}$ for *F. japonica*), except in the case of *Spathiphyllum* ($R^2 = 0.009$, RMSE = 0.0035 $g\,cm^{-2}$), where there was very little overall change in EWT over the experiment (Fig. 1).

Although a strong relationship was found between SNRI and EWT across the combined dataset, there was significant variability in index values across a single leaf sample. Fig. 4 shows the variability in index value across the 25 waveforms retrieved from one leaf sample (the *B. oleracea* leaf). The average (across all time intervals) standard deviation in SNRI across the leaf was 0.095. In comparison, the average standard deviation in SNRI (based on 140 waveforms) for the spectrally uniform Spectralon calibration panel was 0.020, with a maximum standard deviation at any time interval of 0.022, suggesting only a small proportion (23%) of the variability across a leaf could be accounted for by fine-scale temporal variations in laser output intensity. This suggests that there may be significant spatial variability in EWT, or in other factors such as leaf structure which may influence spectral properties, within each leaf and this is discussed in detail in Section 4.

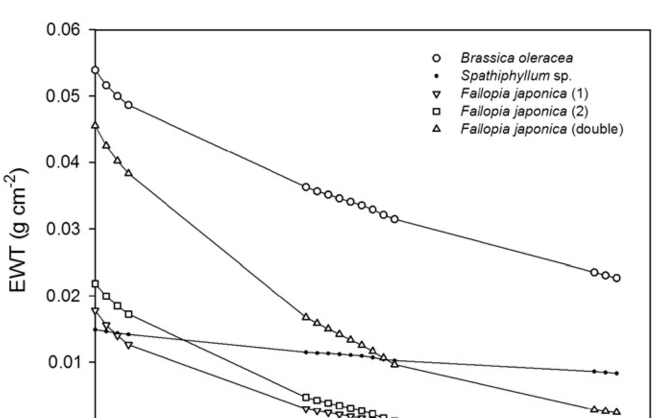

Fig. 1. Change in leaf EWT (g cm^{-2}) over the course of the experiment.

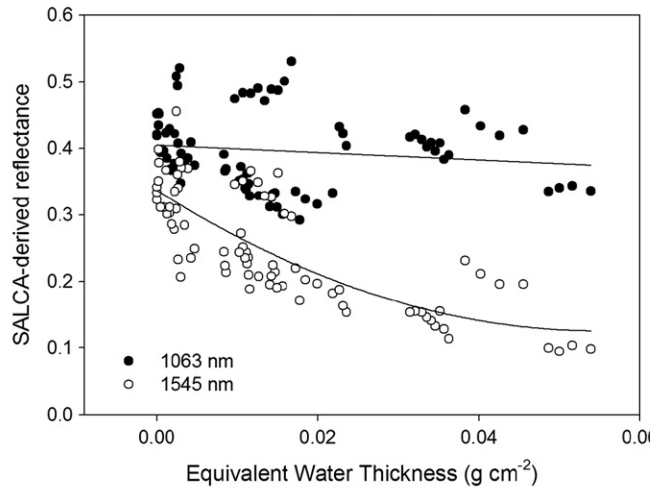

Fig. 2. Change in mean SALCA-derived reflectance of leaf samples with EWT (g cm^{-2}) for the 1063 nm and 1545 nm wavelengths.

To compare the relationship between the SALCA-measured spectral index (SNRI) to that from leaf reflectance modelling, the PROSPECT modelled and experimental data were combined (Fig. 5). The relationship found from the experimental data was similar, and had a similar slope, to that derived from the model. However, the experimental relationship was more linear. In general, most measurements of the SNRI lay within the range expected from PROSPECT. However, there were exceptions related to the leaf sample with double thickness (*F. japonica* (double)) and samples with very low EWT. The measured SNRI for the double leaf sample was generally lower than would be expected for an equivalent EWT. An increase in the leaf structure parameter (N) in PROSPECT was shown previously (Section 3.1) to result in a decrease in the SNRI and as this parameter relates to the leaf anatomy and the number of stacked layers from which it is assumed in the model to be composed (Jacquemoud & Baret, 1990), it is reasonable to assume that the value of N that would be appropriate for modelling two tightly stacked leaves may lie outside of the range considered in the PROSPECT modelling ($N = 1$–3). Changes in leaf structure during drying, and resulting reflectance changes, may also account for differences between modelled and observed SNRI at very low EWT levels and are discussed further in the next section.

4. Discussion

Leaf reflectance modelling using the PROSPECT-5 leaf reflectance model demonstrated that the wavelengths employed by the SALCA instrument (1063 and 1545 nm) are suitable for use in the estimation

Table 5
RMA regression results showing the relationship between SALCA-derived reflectance and spectral indices and EWT (g cm^{-2}) of leaf samples. RMSE values were obtained through model inversion and leave-one-out cross validation.

Dependent variable	Slope	Intercept	R^2	RMSE (g cm^{-2})
SNRI	9.5825**	0.1029	0.7959	0.0069
SSRI	−12.2207**	0.8242	0.7879	0.0070
1545 nm[a]	−1.4144**	0.6450	0.6556	0.0080
1063 nm[a]	−0.7329*	0.707	0.0343	0.0184

[a] X and Y variables square root transformed before regression.
* Significant at a P<0.05 level.
** Significant at a P<0.01 level.

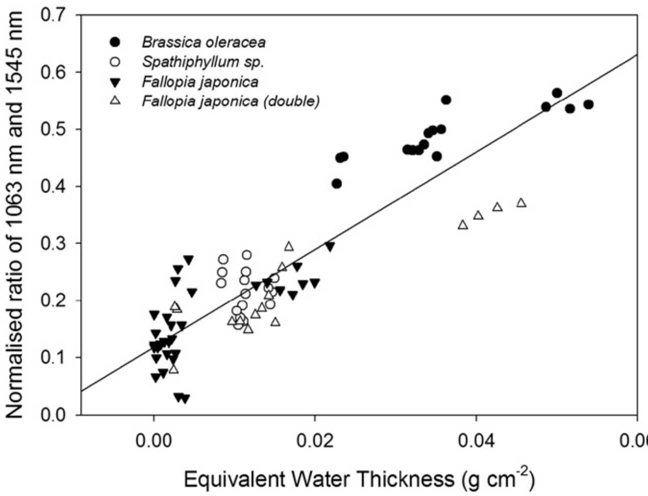

Fig. 3. Relationship between mean SALCA-derived normalised ratio of 1063 and 1545 nm (SNRI) and EWT (g cm^{-2}) of the leaves.

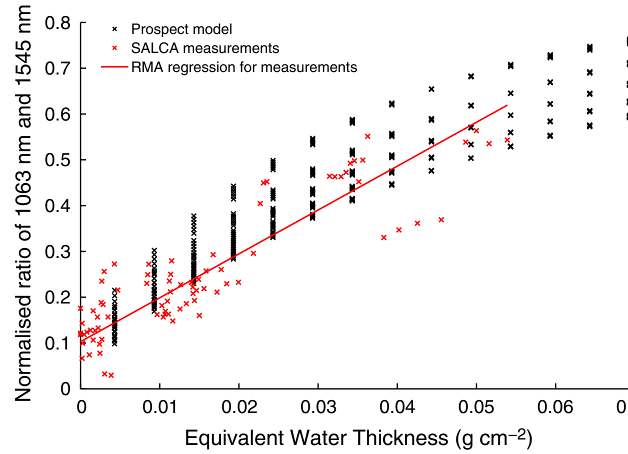

Fig. 5. Comparison of experimental and PROSPECT modelled data relating the SALCA-derived SNRI to the EWT of the leaf.

of leaf EWT. The 1545 nm wavelength was known to lie in a spectral region highly sensitive to leaf moisture content from previous modelling studies (for example, Ceccato et al., 2001). However, the 1063 nm laser is also influenced to some extent by leaf water content, as well as dry matter content and leaf structure (Bowyer & Danson, 2004; Ceccato et al., 2001), and it was unclear to what extent the sensitivity of an index derived from these two wavelengths would be compromised by use of this reference wavelength. The SNRI proposed here was found to have very similar sensitivity to EWT to other indices more commonly used with passive optical data, such as the NDWI, and outperformed some commonly employed ratios (e.g. MSI), due to the greater impact of leaf moisture on 1545 nm reflectance compared to longer wavelengths (1600 nm). A normalised ratio of the two SALCA wavelengths was found to be preferable to a simple ratio, but both would represent effective methods of estimating EWT.

The modelling results indicated that leaf structure (including internal leaf structure and thickness) was likely to influence estimation of EWT using spectral indices at these wavelengths. This influence on spectral indices for estimation of water content has been found in previous studies (for example, Danson et al., 1992; Zarco-Tejada et al., 2003). Ceccato et al. (2001) found that leaf structure accounted for 7.5% of the variation in the Moisture Stress Index. Although the effect is small compared to

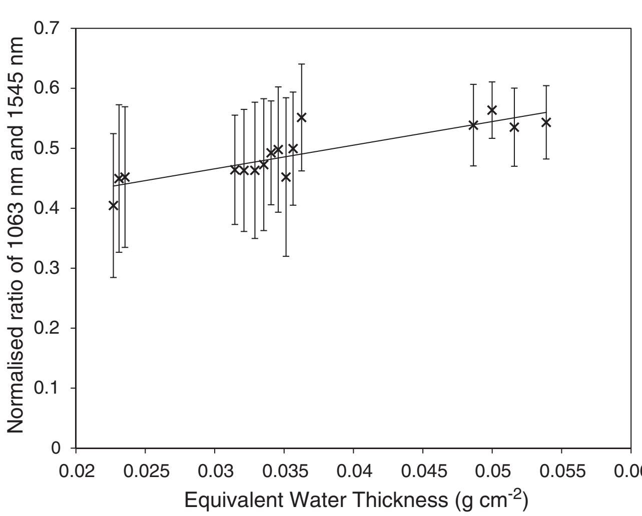

Fig. 4. Relationship between the SALCA-measured SNRI and EWT for the *Brassica oleracea* leaf. Crosses represent the mean index value of the sample waveforms, whilst the error bars show ±1 standard deviation. $R^2 = 0.743$, $n = 25$, $P < 0.001$.

the magnitude of change in the SNRI resulting from varying EWT, it is likely to introduce some error in the estimation of EWT using SALCA. There is no evidence that the SNRI was significantly more influenced by leaf structure than other commonly used indices (e.g. MSI or $ND_{1062,1393}$), but it may be necessary to calibrate the relationship between EWT and SNRI separately for different leaf structures (for example, needle-leaves versus broadleaves).

The experimental results support the outcomes of the PROSPECT modelling and demonstrate that reflectance properties and derived spectral indices can be successfully obtained from active optical measurements with a dual-wavelength laser scanner. The observed trend was more linear than was expected from the PROSPECT model. Sensitivity of middle-infrared based indices to changes in EWT has been shown to decrease at higher levels of EWT (Wu et al., 2012), and as the range of leaf EWT observed during the experiment was limited (0–0.054 g cm^{-2}), a non-linear trend is to be expected over a greater range of EWT. It was also observed that some values of SALCA SNRI at low levels of EWT lay outside of the range predicted by PROSPECT. This result is similar to that demonstrated by Aldakheel and Danson (1997), where a greater difference between PROSPECT modelled and measured spectral reflectance occurred near the end of a leaf dehydration experiment. This was suggested to be due to changes in leaf structure during drying, with a leaf structure parameter (N) of 4.9 needed to produce the measured spectral properties of dry leaves with an EWT of 0.02 g cm^{-2}. This is well outside of the values of N used in modelling here (N = 1–3) and may well account for these discrepancies, which predominantly lie below modelled values. Overall, the strong relationship ($R^2 = 0.8$) between EWT and a normalised ratio of the two SALCA wavelengths (1063 nm and 1545 nm) indicates the potential for using this technology for measuring leaf moisture content in the field, with potential applications in up-scaling physiological measurements, assessing spatial heterogeneity in leaf and canopy water stress and in validation of estimates of leaf moisture content from satellite imagery. The results also point to the future potential of airborne and spaceborne dual-wavelength and multispectral laser scanners for combined three-dimensional measurement of canopy structure and biochemistry.

Despite a strong relationship for the combined leaf data set, a significant spread of spectral values was measured within individual leaves. Measurements of leaves made with a laser with low beam divergence and small footprint size, such as those of SALCA, especially at close range, differ markedly to measurements using a typically wider field-of-view passive sensor. Individual waveforms in this experiment represent the reflectance characteristics of an area of leaf with a diameter of 0.58–0.7 cm, with multiple observations per leaf. SALCA estimates of EWT are therefore made at a within-leaf scale, whilst comparison is made to EWT directly measured for the whole leaf. Leaf blades exhibit fine-scale spatial variability in structure (for example, differences between leaf veins and different areas of the leaf blade) and these structural characteristics have a major influence on the distribution of water across the leaf (Sack & Holbrook, 2006), as well as resulting in variation in leaf thickness (Repka & Jureková, 1981). The rate at which water is lost by transpiration also varies between zones of the leaf blade and higher water saturation deficits may be present at the base and centre of drying leaves (Slavík, 1963). As leaves become water stressed, stomatal conductance decreases and in some leaves, this process can result in a patchy distribution of stomatal closure (patchy stomatal conductance), potentially reducing transpiration from some areas of the leaf (Kamakura et al., 2012; Mott & Buckley, 2000). Under high levels of water stress, vein cavitation can also occur, limiting water supply to parts of a leaf blade (Nardini et al., 2003; Scoffoni et al., 2011). As EWT is determined by cell water content and leaf thickness, the variability in these parameters across the leaf, due to the processes described above, may account for variability in reflectance between SALCA footprints. Variability in spectral properties at other wavelengths has been previously detected at a within-leaf scale, and especially over leaf veins (Castro-Esau et al., 2006). A patchy pattern of drying was visible in many of the leaf samples during the experiment; however, further research is needed to determine the degree to which patchy distribution of leaf moisture accounts for this variability compared to other potential sources of noise. Comparison with variation in SNRI across a Spectralon panel demonstrated fine temporal variations in laser output intensity or background illumination were unlikely to account for much of the variability observed within leaves. However, although reflectance measurements obtained from active laser instruments will be less influenced by illumination and viewing geometry than those of passive hyperspectral sensors, the signal-to-noise ratio of laser intensity measurements may often be lower, as the reflected signal is recorded in narrow time bins (for example, signal-to-noise ratios in this experiment were between 8.87 dB and 12.88 dB). The signal-to-noise characteristics will also change according to range and can be modified through the use of filters or through adjusting laser output power. More extensive research on the signal-to-noise characteristics of active laser instruments is therefore needed in order to assess the precision with which leaf and canopy reflectance properties can be derived.

This paper focussed on estimation of EWT from dual-wavelength laser scanner intensity measurements at the scale of individual leaves. However, the majority of applications for this technology, for example in disease or drought stress detection, require estimates at an individual tree or canopy scale. To date, no studies have examined the potential of dual-wavelength or multispectral laser scanning in estimating vegetation biochemical properties at a canopy scale. However, there are some important implications of working at such scales which should be recognised. Eitel et al. (2006) demonstrated that relationships between spectral indices and plant water status were weaker for canopy than for leaf scales. They gave variability in background reflectance and leaf area index as potential reasons. Laser scanner data, by combining reflectivity measurements with range measurements have the potential to supress the influence of the background soil or understorey, and to directly measure and account for structural variability, such as changes in LAI.

A number of potential challenges to estimating leaf moisture over canopy scales exist. This study has examined only laser waveforms in which the entire laser footprint is occupied by leaf material at a single range. The reality in a tree canopy will be more complex, with some returns representing partial ‘edge’ hits and others resulting from full or partial hits of woody material. Returns from woody material should have low values of the SNRI. For example, ASD spectroradiometer contact probe measurements of bark samples from five UK tree species, made in support of this research, gave a mean SNRI of 0.07 compared to an SNRI of 0.1 or greater for the majority of leaf samples measured here. It should therefore be possible to separate returns from woody material from those of live leaves. However, index values for bark may be quite variable, depending on, for example the presence of lichen and moss. It may also be difficult to separate returns from woody canopy elements from those from dead or very dry leaves. However, for many applications, where the primary interest would be in detecting the early stages of leaf water stress, this may not present a major limitation. Of greater concern, will be accounting for the influence of objects only partially occupying the laser beam footprint. The SNRI value should be relatively insensitive to the cross section of the target within the laser footprint for the first return in the waveform. However, one advantage of full waveform laser scanner data, such as that provided by SALCA, is that multiple returns can be recorded from different depths in the canopy. To determine the reflectivity and biochemical properties of second and subsequent targets, the reduction in transmitted energy incident on the target will need to be taken into account, if this differs for the two spectral bands. Where more than one material (such as both leaf and woody material) occurs in the laser footprint within the same range bin, estimates of biochemical parameters may also be biased. The likelihood of this occurring seems likely to be influenced by canopy structure and leaf size, shape and orientation. A further source of error results from the small offset in footprint position between the two wavelengths for the SALCA instrument. Whilst this represents an offset of approximately 1% of the footprint area, there will be some level of noise introduced related to both the amount of material (for partial hits) and the potential differences in leaf structure between footprints and further work is needed to fully characterise this error. Analysis at canopy scales could be limited to single returns to minimise this influence or averaged within voxels. Finally, as with passive optical approaches, estimation of biochemical properties at canopy scales may also be influenced by variation in tree species and to some extent atmospheric conditions and background illumination. Research is on-going to determine the potential for applying the dual-wavelength laser scanner methods described here to the retrieval of estimates of moisture content at canopy scales, and to examine the potential for making similar measurements from an airborne platform.

5. Conclusions

This study demonstrates experimentally the potential of dual-wavelength laser scanning for estimating leaf moisture content. Using intensity measurements from the Salford Advanced Laser Canopy Analyser, a strong relationship was found between a laser-measured spectral index (SALCA Normalised Ratio Index, SNRI) and leaf EWT. These results show potential for the use of dual-wavelength and multispectral laser scanner data for measuring the three-dimensional distribution of vegetation biochemical properties, for the monitoring of vegetation vigour and to provide a means of up-scaling leaf-level physiological measurements to canopy scales. Further research is necessary to examine whether relationships hold at canopy scales, and to develop approaches to utilise three dimensional estimates of biochemical properties in the validation of other remotely sensed data and in ecological modelling.

Acknowledgements

The development and initial testing of the SALCA instrument was funded by a Technology Proof-of-Concept Grant (NE/H002685/1) and a Small Project Grant (NE/I01702X/1) from the Natural Environment Research Council, UK.

References

Ahokas, E., Kaasalainen, S., Hyyppä, J., & Suomalainen, J. (2006). Calibration of the Optech ALTM 3100 laser scanner intensity data using brightness targets. *The International Archives of the Photogrammetry, Remote Sensing and Spatial Information Sciences*, *36*(A1) (CD-ROM).

Aldakheel, Y. Y., & Danson, F. M. (1997). Spectral reflectance of dehydrating leaves: Measurements and modelling. *International Journal of Remote Sensing*, *18*, 3683–3690.
Allen, C. D., Macalady, A. K., Chenchouni, H., Bachelet, D., McDowell, N., Vennetier, M., et al. (2010). A global overview of drought and heat-induced tree mortality reveals emerging climate change risks for forests. *Forest Ecology and Management*, *259*, 660–684.
Asner, G. P. (1998). Biophysical and biochemical sources of variability in canopy reflectance. *Remote Sensing of Environment*, *64*, 234–253.
Asner, G. P., Knapp, D. E., Jones, M. O., Kennedy-Bowdoin, T., Martin, R. E., Boardman, J., et al. (2007). Carnegie Airborne Observatory: In-flight fusion of hyperspectral imaging and waveform light detection and ranging (wLiDAR) for three-dimensional studies of ecosystems. *Journal of Applied Remote Sensing*, *1*, 013536.
Bowyer, P., & Danson, F. M. (2004). Sensitivity of spectral reflectance to variation in live fuel moisture content at leaf and canopy level. *Remote Sensing of Environment*, *92*, 297–308.
Castro-Esau, K. L., Sánchez-Azofeita, G. A., Rivard, B., Wright, S. J., & Quesda, M. (2006). Variability in leaf optical properties of Mesoamerican trees and the potential for species classification. *American Journal of Botany*, *93*, 517–530.
Ceccato, P., Flasse, S., Tarantola, S., Jacquemoud, S., & Grégoire, J. M. (2001). Detecting vegetation water content using reflectance in the optical domain. *Remote Sensing of Environment*, *77*, 22–33.
Danson, F. M., & Bowyer, P. (2004). Estimating live fuel moisture content from remotely sensed reflectance. *Remote Sensing of Environment*, *92*, 309–321.
Danson, F. M., Steven, M. D., Malthus, T. J., & Clark, J. A. (1992). High-spectral resolution data for determining leaf water content. *International Journal of Remote Sensing*, *13*, 461–470.
Dawson, T. P., North, P. R. J., Plummer, S. E., & Curran, P. J. (2003). Forest ecosystem chlorophyll content: Implications for remotely sensed estimates of net primary productivity. *International Journal of Remote Sensing*, *24*, 611–617.
Eitel, J. U. H., Gessler, P. E., Smith, A. M. S., & Robberecht, R. (2006). Suitability of existing and novel spectral indices to remotely detect water stress in *Populus* spp. *Forest Ecology and Management*, *229*, 170–182.
Eitel, J. U. H., Vierling, L. A., & Long, D. S. (2010). Simultaneous measurement of plant structure and chlorophyll content in broadleaf saplings with a terrestrial laser scanner. *Remote Sensing of Environment*, *114*, 2229–2237.
Eitel, J. U. H., Vierling, L. A., Long, D. S., & Hunt, E. R. (2011). Early season remote sensing of wheat nitrogen status using a green scanning laser. *Agricultural and Forest Meteorology*, *151*, 1338–1345.
Féret, J. -B., François, C., Asner, G. P., Gitelson, A., Martin, R. E., Bidel, L. P. R., et al. (2008). PROSPECT-4 and 5: Advances in the leaf optical properties model separating photosynthetic pigments. *Remote Sensing of Environment*, *112*, 3030–3043.
Féret, J. -B., François, C., Gitelson, A., Asner, G. P., Barry, K. M., Panigada, C., et al. (2011). Optimizing spectral indices and chemometric analysis of leaf chemical properties using radiative transfer modelling. *Remote Sensing of Environment*, *115*, 2742–2750.
Gao, B. (1996). NDWI — A normalized difference water index for remote sensing of vegetation liquid water from space. *Remote Sensing of Environment*, *58*, 257–266.
Gu, Y., Brown, J. F., Verdin, J. P., & Wardlow, B. (2007). A five-year analysis of MODIS NDVI and NDWI for grassland drought assessment over the central Great Plains of the United States. *Geophysical Research Letters*, *34*, L06407.
Hakala, T., Suomalainen, J., Kaasalainen, S., & Chen, Y. (2012). Full waveform hyperspectral LiDAR for terrestrial laser scanning. *Optics Express*, *20*, 7119–7127.
Höfle, B., & Pfeifer, N. (2007). Correction of laser scanning intensity data: Data and model-driven approaches. *ISPRS Journal of Photogrammetry and Remote Sensing*, *62*, 415–433.
Huete, A. R., Jackson, R. D., & Post, D. F. (1985). Spectral response of a plant canopy with different soil backgrounds. *Remote Sensing of Environment*, *17*, 37–53.
Hyyppä, J., Hyyppä, H., Leckie, D., Gougeon, F., Yu, X., & Maltamo, M. (2008). Review of methods of small-footprint airborne laser scanning for extracting forest inventory data in boreal forests. *International Journal of Remote Sensing*, *29*, 1339–1366.
Jacquemoud, S., & Baret, F. (1990). PROSPECT: A model of leaf optical properties spectra. *Remote Sensing of Environment*, *34*, 75–91.
Kaasalainen, S., Krooks, A., Kukko, A., & Kaartinen, H. (2009). Radiometric calibration of terrestrial laser scanners with external reference targets. *Remote Sensing*, *1*, 144–158.
Kamakura, M., Kosugi, Y., Takanashi, S., Tobita, H., Uemura, A., & Utsugi, H. (2012). Observation of the scale of patchy stomatal behavior in leaves of *Quercus crispula* using an Imaging-PAM chlorophyll fluorometer. *Tree Physiology*, *32*, 839–846.
Kim, S., Hinckley, T., & Briggs, D. (2011). Classifying individual tree genera using stepwise cluster analysis based on height and intensity metrics derived from airborne laser scanner data. *Remote Sensing of Environment*, *115*, 3329–3342.
Korpela, I. S. (2008). Mapping of understory lichens with airborne discrete-return LiDAR data. *Remote Sensing of Environment*, *112*, 3891–3897.
Meentemeyer, R. K., Anacker, B. L., Mark, W., & Rizzo, D. M. (2008). Early detection of emerging forest disease using dispersal estimation and ecological niche modelling. *Ecological Applications*, *18*, 377–390.
Morsdorf, F., Nichol, C., Malthus, T., & Woodhouse, I. H. (2009). Assessing forest structural and physiological information content of multispectral LiDAR waveforms by radiative transfer modelling. *Remote Sensing of Environment*, *113*, 2152–2163.
Mott, K. A., & Buckley, T. N. (2000). Patchy stomatal conductance: Emergent collective behaviour of stomata. *Trends in Plant Science*, *5*, 258–262.
Narayanan, R. M., & Pflum, M. T. (1999). Remote sensing of vegetation stress and soil contamination using CO_2 laser reflectance ratios. *International Journal of Infrared and Millimeter Waves*, *20*, 1593–1617.
Nardini, A., Salleo, S., & Raimondo, F. (2003). Changes in leaf hydraulic conductance correlate with vein embolism in *Ceris siliquastrum* L. *Trees*, *17*, 529–534.
Nepstad, D. C., Stickler, C. M., Soares-Filho, B., & Merry, F. (2008). Interactions among Amazon land use, forests and climate: Prospects for a near-term forest tipping point. *Philosophical Transactions of the Royal Society B-Biological Sciences*, *363*, 1737–1746.
Notarnicola, C., & Posa, F. (2007). Inferring vegetation water content from C- and L-band SAR images. *IEEE Transactions on Geoscience and Remote Sensing*, *45*, 3165–3171.
Ørka, H. O., Næsset, E., & Bollandsås, O. M. (2009). Classifying species of individual trees by intensity and structure features derived from airborne laser scanner data. *Remote Sensing of Environment*, *113*, 1163–1174.
Peterson, S. H., Roberts, D. A., & Dennison, P. E. (2008). Mapping live fuel moisture with MODIS data: A multiple regression approach. *Remote Sensing of Environment*, *112*, 4272–4284.
Rall, J., & Knox, R. (2004). Spectral ratio biospheric lidar. *22nd International Laser Radar Conference (ILRC 2004), Proceedings of the Conference held 12–16 July 2004 in Matera, Italy ESA SP-561* (pp. 831). Paris: European Space Agency.
Repka, J., & Jureková, Z. (1981). Heterogeneity of the Maize leaf blade in photosynthetic characteristics, respiration, mineral nutrient contents, and growth substances. *Biologia Plantarum*, *23*, 145–155.
Rock, B. N., Vogelmann, J. E., Williams, D. L., Vogelmann, A. F., & Hoshizaki, T. (1986). Remote detection of forest damage. *Bioscience*, *36*, 439–445.
Rodríguez-Pérez, J. R., Riaño, D., Carlisle, E., Ustin, S., & Smart, D. R. (2006). Evaluation of hyperspectral reflectance indexes to detect grapevine water status in vineyards. *American Journal of Enology and Viticulture*, *58*, 302–317.
Sack, L., & Holbrook, N. M. (2006). Leaf hydraulics. *Annual Review of Plant Biology*, *57*, 361–381.
Scoffoni, C., Rawls, M., McKown, A., Cochard, H., & Sack, L. (2011). Decline of leaf hydraulic conductance with dehydration: Relationship to leaf size and venation architecture. *Plant Physiology*, *156*, 832–843.
Skakun, R. S., Wulder, M. A., & Franklin, S. E. (2003). Sensitivity of the thematic mapper enhanced wetness difference index to detect mountain pine beetle red-attack damage. *Remote Sensing of Environment*, *86*, 433–443.
Slavík, B. (1963). The distribution pattern of transpiration rate, water saturation deficit, stomata number and size, photosynthetic and respiration rate in the area of the tobacco leaf blade. *Biologia Plantarum*, *5*, 143–153.
Smith, R. J. (2009). Use and misuse of the Reduced Major Axis for line-fitting. *American Journal of Physical Anthropology*, *140*, 476–486.
Sturrock, R. N., Frankel, S. J., Brown, A. V., Hennon, P. E., Kliejunas, J. T., Lewis, K. J., et al. (2011). Climate change and forest diseases. *Plant Pathology*, *60*, 133–149.
Tan, S., Narayanan, R. M., & Shetty, S. K. (2005). Polarized LiDAR reflectance measurements of vegetation at near-infrared and green wavelengths. *International Journal of Infrared and Millimeter Waves*, *26*, 1175–1194.
Thomson, S. J., Oullet-Plamondon, C. M., DeFauw, S. L., Huang, Y., Fisher, D. K., & English, P. J. (2012). Potential and challenges in use of thermal imaging for humid region irrigation system management. *Journal of Agricultural Science*, *4*, 103–116.
Van der Zande, D., Mereu, S., Nadezhdina, N., Cermak, J., Muys, B., Coppin, P., et al. (2009). 3D up-scaling of transpiration from leaf to tree using ground-based LiDAR: Application on a Mediterranean Holm oak (*Quercus ilex* L.) tree. *Agricultural and Forest Meteorology*, *149*, 1573–1583.
Van Leeuwen, M., & Nieuwenhuis, M. (2010). Retrieval of forest structural parameters using LiDAR remote sensing. *European Journal of Forest Research*, *129*, 749–770.
Wang, Q., & Li, P. (2012). Identification of robust hyperspectral indices on forest leaf water content using PROSPECT simulated dataset and field reflectance measurements. *Hydrological Processes*, *26*, 1230–1241.
Wang, P. J., Xie, D. H., Zhang, J. H., & Xu, Y. (2012). Inversion of winter wheat water content with the relationship between canopy parameters and spectra based on different irrigations. *Spectroscopy and Spectral Analysis*, *32*, 209–213.
Wei, G., Shalei, S., Bo, Z., Shuo, S., Faquan, L., & Xuewu, C. (2012). Multi-wavelength canopy LiDAR for remote sensing of vegetation: Design and system performance. *ISPRS Journal of Photogrammetry and Remote Sensing*, *69*, 1–9.
Wessman, C. A. (1994). Estimating canopy biochemistry through imaging spectrometry. In J. Hill, & J. Megier (Eds.), *Imaging spectrometry — A tool for environmental observations. Eurocourses: Remote sensing*. Netherlands: Springer.
Woodhouse, I. H., Nichol, C., Sinclair, P., Jack, J., Morsdorf, F., Malthus, T., et al. (2011). A multispectral canopy LiDAR demonstrator project. *IEEE Geoscience and Remote Sensing Letters*, *8*, 839–843.
Wu, J., Zhang, J., Lu, A., & Zhou, L. (2012). An exploratory analysis of spectral indices to estimate vegetation water content using sensitivity function. *Remote Sensing Letters*, *3*, 161–169.
Yi, Q. X., Bao, A. M., Luo, Y., & Zhao, J. (2012). Measuring cotton water status using water-related vegetation indices at leaf and canopy levels. *Journal of Arid Land*, *4*, 310–319.
Zarco-Tejada, P. J., Rueda, C. A., & Ustin, S. L. (2003). Water content estimation in vegetation with MODIS reflectance data and model inversion methods. *Remote Sensing of Environment*, *85*, 109–124.